

Access to this work was provided by the University of Maryland, Baltimore County (UMBC) ScholarWorks@UMBC digital repository on the Maryland Shared Open Access (MD-SOAR) platform.

Please provide feedback

Please support the ScholarWorks@UMBC repository by emailing scholarworks-group@umbc.edu and telling us what having access to this work means to you and why it's important to you. Thank you.

PROCEEDINGS OF SPIE

[SPIDigitalLibrary.org/conference-proceedings-of-spie](https://spiedigitallibrary.org/conference-proceedings-of-spie)

Deep-UV standoff Raman spectroscopy

Bradley R. Arnold, Eric Bowman, Leslie Scheurer

Bradley R. Arnold, Eric Bowman, Leslie Scheurer, "Deep-UV standoff Raman spectroscopy," Proc. SPIE 10983, Next-Generation Spectroscopic Technologies XII, 109830H (13 May 2019); doi: 10.1117/12.2519033

SPIE.

Event: SPIE Defense + Commercial Sensing, 2019, Baltimore, Maryland, United States

Deep-UV standoff Raman spectroscopy

Bradley R. Arnold, Eric Bowman, and Leslie Scheurer

Department of Chemistry and Biochemistry
University of Maryland Baltimore County
1000 Hilltop Circle
Baltimore, MD. 21250

ABSTRACT

The availability of high peak-power laser systems capable of delivering intense deep-UV pulses has brought renewed interest in using Raman spectroscopy as both a selective and sensitive analytical technique for stand-off detection. Our approach uses a high power pulsed-laser as the excitation source, specifically the fourth and fifth harmonics of a Nd:YAG laser. One of the hurdles to be overcome to allow deep-UV Raman spectroscopy to become accessible is a direct method of calibrating both the observation frequency and detector response of the spectrograph being used. This report outlines our efforts to understand the photochemical and photophysical consequences of high-peak power excitation of cyclohexane for potential use as a secondary Raman standard in the deep-UV. Evaluation of the photochemical stability, both from multi-photon absorption and in the presence or absence of dissolved oxygen as well as the possibility of (near) resonance enhancement of the C-H stretching region will be described.

Key Words: cyclohexane, Raman calibration, secondary standard, resonance enhancement, spectral simulation.

INTRODUCTION

The availability of high peak-power laser systems capable of delivering intense deep-UV pulses has brought renewed interest into using Raman spectroscopy as an analytical technique for stand-off detection.¹⁻⁵ Given that Raman scattering cross-sections are one billion times smaller than typical fluorescence cross-sections, overcoming the nine orders of magnitude decrease in sensitivity is a daunting challenge that remains to be addressed.⁷⁻¹⁰ One strategy to increase Raman scattering cross-sections is to use UV photons as the scattering source. The frequency dependence of the differential cross-sections is usually defined using a simple λ^4 dependence,¹¹ particularly when the incident excitation frequency is much lower than the frequency required to reach electronic excited states. Thus, cross-sections observed using the fifth harmonic of Nd:YAG at 213 nm will be between 40 to 50 times greater than those observed using the second harmonic at 532 nm based solely on the λ^4 dependence. When the incident wavelength approaches the energy needed for electronic excitation of the scattering molecule the possibility of resonance enhancement factors of $10^2 - 10^6$ could be an attractive solution to the Raman sensitivity issue.⁷⁻¹⁰

Moving into resonance with electronic transitions is not without potential drawbacks; the loss of intensity in both the incident and scattered beams due to absorption by the sample is a significant difficulty that will need to be overcome. In addition to losses due to absorption, interference by fluorescence and photochemical degradation of the sample are among the consequences to be considered when exciting near resonance with electronic transitions. Thus, there are several potential pitfalls that are unique to deep-UV excitation in Raman experiments that are not encountered when visible and near-IR excitation sources are used.

Our approach to deep-UV Raman uses a high power pulsed laser, specifically the fourth and fifth harmonics of a Nd:YAG laser, coupled with an intensified charge coupled device (ICCD) detection system to obtain Raman spectra. The high peak powers of the incident pulses result in significant scattered intensity at wavelengths where the detector quantum efficiency is high. For UV excitation wavelengths, the entire Raman spectrum occurs within ca 20 nm of the incident radiation. Fluorescence emission, both from the analyte and background sources, generally occurs at longer wavelengths such that these background emission sources do not interfere with the observation of Raman scattering.

One of the hurdles to be overcome to allow deep-UV Raman spectroscopy to become accessible is a direct method of calibrating both the observation frequency and detector response profiles of the spectrograph being used. Typical methods utilize expensive calibration light sources that require frequent recalibration to be accurate. Other methods include the possibility of using secondary standards but, to date, there are no accepted standards for use at excitation wavelengths below 488 nm. To be viable as a secondary standard the material should be inexpensive to obtain in high purity and readily available; be photochemically stable and, ideally, free from complex measurement effects. This report outlines our efforts to understand the photochemical and photophysical consequences of high-peak power excitation of cyclohexane for potential use as a Raman standard in the deep-UV. Evaluation of the photochemical stability, both from multi-photon absorption and in the presence or absence of dissolved oxygen as well as the possibility of (near) resonance enhancement of the C-H stretching region are described in detail.

EXPERIMENTAL

Spectroscopy experiments were carried out on HPLC grade cyclohexane placed into a 1 cm quartz cuvette and purged with a stream N₂ gas for at least 10 minutes to remove oxygen. Many solvents, including cyclohexane, have a significant interaction with dissolved oxygen resulting in the appearance of absorption in the UV wavelength range.¹⁴ Purging with N₂ gas removes this residual absorption and mitigates possible photochemical decomposition processes in these samples.¹⁵ The UV-visible spectrum of each sample was collected before and after irradiation. Laser pulses of 213-nm laser light were generated with a Brilliant b pulsed nanosecond Nd:YAG laser operating at 10 Hz equipped with the commercial doubling, quadrupling or quintupling crystal series to obtain the second, fourth or fifth harmonic, respectively, from a 1064-nm fundamental. The full spectrometer setup is depicted in Figure 1.

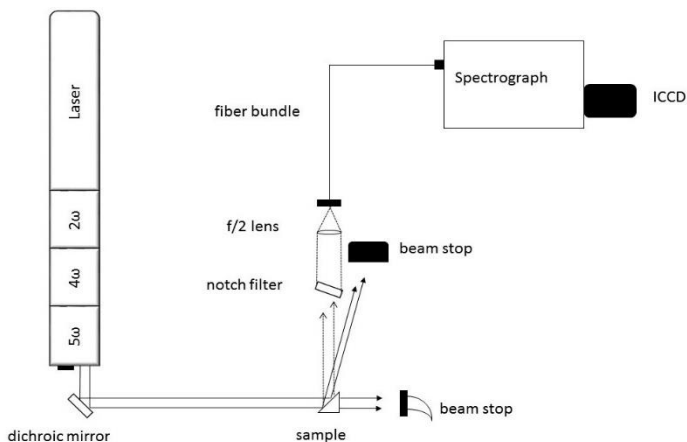


Figure 1. Schematic of the UV Raman spectrometer in which 213-nm light was generated as the fifth harmonic of a pulsed nanosecond Nd:YAG laser. Unfocused laser was directed onto the sample using dichroic mirrors. The specular beam was directed away from the collection optic and into a beam stop by tilting the sample slightly. Scattered light (dotted lines) was collected perpendicular to the incident beam. A notch filter was used to reject the scattered laser frequency. A quartz lens was used to focus a collimated beam into the fiber bundle attached to the spectrograph/detector system.

Rejection of unwanted harmonics was carried out using dichroic mirror sets yielding an average power of 5 mJ laser light per pulse at each of the wavelengths studied. Each fundamental was arranged to allow vertically polarized laser light to strike the sample and thus simplify polarization effects in the observed spectra. The laser beam was left unfocused and the incident 8-mm diameter beam was directed onto the hypotenuse of the triangular quartz cuvette to induce scatter. The Raman scatter was collected at 90° with respect to the laser pulse and the cuvette face was angled slightly to allow the specular reflection of the laser to avoid the detection system and collection optics.

The scattered light passed through a 213-nm notch filter placed approximately 200 mm from the sample. The filtered scattered light was then coupled using a 25.4-mm f/2 quartz lens into a fiber bundle containing 19 individual 200- μ m fibers rated to transmit from 190 to 1100 nm. The lens was placed approximately 225 mm from the sample and

one focal length (51 mm) from the fiber bundle end. The sample, filter, lens and fiber were held in a one inch ThorLabs cage system. The distal end of the fiber was attached to an Acton 0.3 m spectrograph utilizing a 2400 l/mm grooved grating blazed at 240 nm. The light was detected using a PI MAX intensified charge coupled device (ICCD) cooled to -25°C . Raman spectra were generated by gating of the ICCD using a 10 ns gate controlled by the Winspec 32 software. UV absorption spectra were collected on a Beckman DU640 UV-visible spectrometer.

RESULTS

Absorption spectra for N_2 -purged, air saturated, and O_2 -purged samples of cyclohexane are shown in Figure 2 (upper panel). Figures 3 and 4 include examples of absorption spectra taken of N_2 purged samples before and after excitation with 266 and 213-nm light, respectively. Also shown (Figure 5) is a low-resolution Raman spectrum of cyclohexane obtained using 213-nm light. High-resolution Raman spectra of the C-H stretching region obtained using 532, 266, and 213 -nm excitation wavelengths are shown in Figure 6. These spectra were collected using ca 5 mJ pulses of excitation light at 10 Hz repetition rates for 1800 pulses. The ICCD detector was gated for the 10 ns corresponding to the maximum intensity of the laser pulse.

DISCUSSION

As noted above, for cyclohexane to be viable as a secondary standard for calibration of Raman spectrometers it should be inexpensive to obtain in high purity and readily available; be photochemically stable and, ideally, free from complex measurement effects. Clearly, cyclohexane is inexpensive and readily available, and it has the added benefit of a long shelf-life, but is it photochemically stable and free from complex measurement effects?

It has been well documented that molecular oxygen forms complexes with hydrocarbons.¹⁵ These complexes have been identified through a red-shifted absorption as shown in Figure 2. Little is known about the exact nature of these complexes, but they are presumably charge transfer in nature. The measured optical density of the complex at 220 nm is dependent upon the partial pressure of molecular oxygen suggesting simple complexes being reversibly formed between cyclohexane as solvent and a single oxygen molecule.

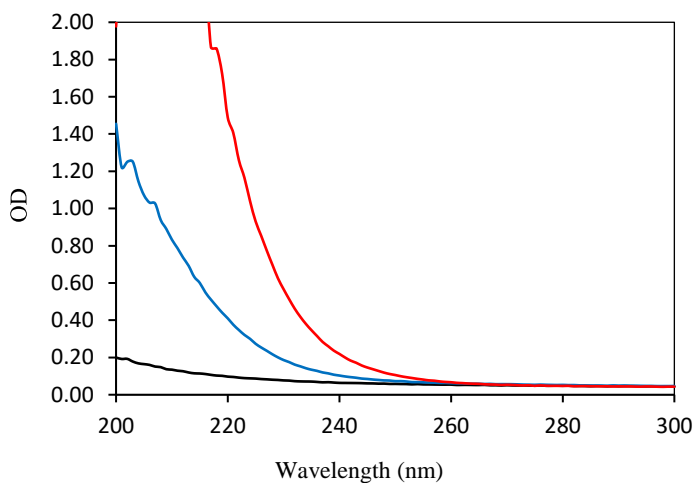


Figure 2. UV-VIS absorbance spectra of cyclohexane samples with increasing concentrations of oxygen. Samples were purged with nitrogen (black), air saturated (blue), or purged with oxygen (red).

The photochemical stability of N_2 purged samples was also studied as shown in Figure 3 and 4. High fluence UV excitation of cyclohexane does lead to product formation. In the case of 266-nm excitation, 50 mJ pulses leads to a photoproduct that has an absorption maximum at 208 nm which is consistent with cyclohexene formation (Figure 3). The formation of cyclohexene as the major (sole) product was confirmed by GC analysis through comparison with authentic samples. The fluence dependence shows clear quadratic behavior indicative of a two-photon process. The deep-UV photolysis of cyclohexane has been studied previously confirming cyclohexene as a major product, but the multi-photon behavior has not been reported previously.

Photolysis of cyclohexane using 213-nm pulses was also studied (Figure 4). In this case, secondary photoproducts, consistent with aromatic hydrocarbons, were produced along with cyclohexene. Presumably, two-

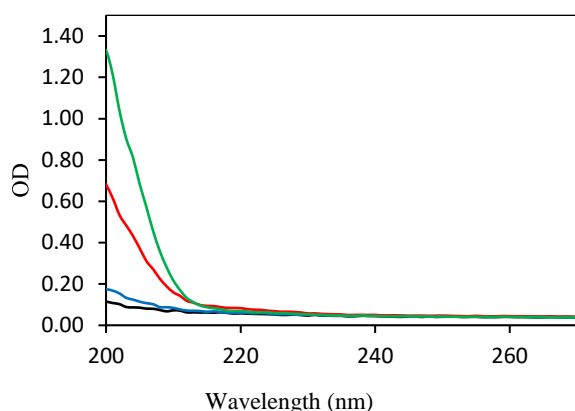


Figure 3. UV-VIS absorbance spectra of nitrogen-purged cyclohexane (black) irradiated for three minutes using 266 nm excitation at 10 mJ (blue), 30 mJ (red), and 50 mJ (green).

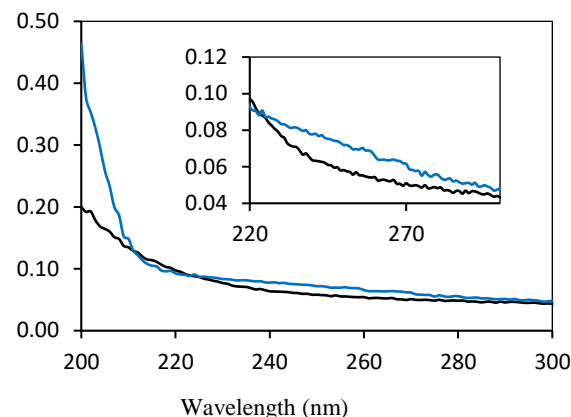


Figure 4. UV-VIS absorbance spectra of nitrogen-purged cyclohexane irradiated using 213 nm excitation at 5 mJ per pulse. The inlaid figure shows evidence of vibrational fine structure, indicating additional photoproducts.

photon excitation of cyclohexane leads to the production of cyclohexene and hydrogen gas. Because the cyclohexene absorption cross-section is large at 213 nm, subsequent single photon events lead to additional conjugation and eventually aromatic compound production either through direct photolysis or by a combination of photochemical and thermal processes. Detailed mechanistic study of these processes is outside the scope of the present report. Germaine to this study however is that it is important to purge these samples to remove oxygen and that the fluence used to excite scatter from them should be limited to less than 5 mJ per pulse to minimize multi-photon photoproducts.

The Raman spectrum of cyclohexane recorded using 213-nm laser excitation is shown in Figure 5. The spectrum is comparable to that published using visible and UV excitation wavelengths with eight major bands being observed.¹¹ Visual comparison of the spectrum with the published¹ spectrum using excitation at 270 nm shows distinct similarities. Unfortunately, the C-H stretching region was not included in the earlier published report. The measured peak intensities collected in Table 1 can be compared with expected values based on published data using visible excitation through the application of equation 1.^{11,23}

$$\frac{\beta_i(\nu_j)}{\beta_{C-H}(\nu_j)} = \frac{\beta_i(\nu_{532})}{\beta_{C-H}(\nu_{532})} \frac{(\nu_j - \nu_i)^3 (\nu_{532} - \nu_{C-H})^3}{(\nu_j - \nu_{C-H})^3 (\nu_{532} - \nu_i)^3} \quad (1)$$

Here the Raman scattering cross-section at the excitation frequency, ν_j , for a single transition, $\beta_R(\nu_j)$, is given relative to the cross-section for C-H stretch $\beta_{C-H}(\nu_j)$ collected using the relative intensities of these same two transitions collected using 532-nm light and scaling according to the ν_j^4 frequency dependence. Such comparisons among these values reveal reasonable agreement for all transitions recorded. This agreement is somewhat surprising due to the extensive extrapolation needed to estimate deep UV cross-sections from the known cross-sections measured in the visible. The relative intensities are well within the reported errors for the available data and are generally within the scatter observed for the published reports.

There are two reports^{19,20} of Raman cross-section determinations using UV sources that examine the possibility of resonance enhancement at these wavelengths. The possibility of enhancement of the C-C stretch at 802 cm^{-1} band was explored¹⁹ but it was determined that the frequency dependence of this transition follows the ν^4 intensity variation closely. It was concluded that this band does not experience significant (pre)resonance enhancement, as supported by the observed intensity pattern described above. This initial report¹⁹ also concluded that the C-H stretching region experienced significant resonance enhancement. The wavelength dependence of the intensities of the C-H stretching vibrations can be used to calculate the expected relative intensities for both

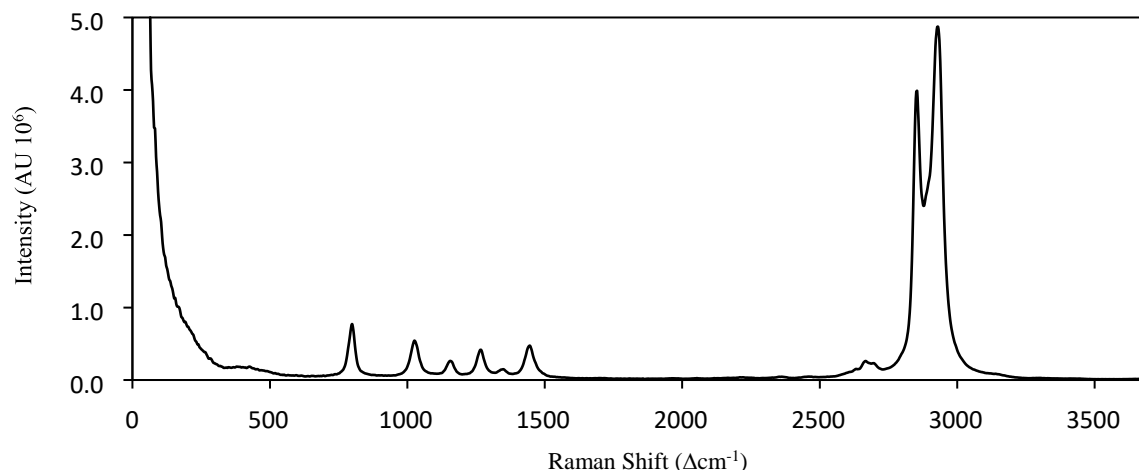


Figure 5. Raman spectrum of cyclohexane collected using 213-nm excitation pulses. Relative intensities were corrected for spectrometer response.

Table 1. Raman transition frequencies, assignments, and relative intensities.

#	Assignment ^a	Freq ^b (lit) (cm ⁻¹)	Intensity ^c (rel)	$\beta_i(\nu_{532})^d$ (lit.)
Cyclohexane				
ν_1	a_{1g} CH ₂ a str	2930 (2930)	1.00	12.8 ^e
ν_2	a_{1g} CH ₂ s str	2854 (2852)	-	17.2
ν_4	a_{1g} CH ₂ rock	1155 (1157)	0.020	
ν_5	a_{1g} CC str	799 (802)	0.070	0.70 ^f
ν_{19}	e_g CH ₂ scis	1446 (1443)	0.052	
ν_{20}	e_g CH ₂ wag	1350 (1347)	0.015	
ν_{21}	e_g CH ₂ twist	1266 (1266)	0.044	
ν_{22}	e_g CC str	1025 (1027)	0.065	

^a assignments based on Ref 10. Frequencies observed in this work are considered accurate to 4 cm⁻¹, literature values from Ref 10. ^c relative intensities in energy units. ^d collected literature values of differential Raman cross-sections adjusted to 213 nm. ^e Ref 14. ^f Ref 15.

the C-C and C-H stretches. The calculated ratio for the integrated C-H stretching region relative to the C-C stretch at 802 cm⁻¹ is about 20 based on these two reports.^{19,20} It is of interest that using the cross-sections for cyclohexane that have been reported^{11,23} using a visible excitation source at 785 nm, and assuming no resonance contributions to the observed intensities, the relative intensity of these two transitions should be approximately 10. The current data suggests a relative intensity that is intermediate between these two estimates at close to 14. We conclude that any resonance enhancement effects in the cyclohexane spectra are a relatively small contribution to the observed cross section.

To fully assess the possibility of resonance enhancement in the UV spectra of cyclohexane the wavelength dependence of the cross-sections was measured using 532, 266, and 213-nm laser excitation. Figure 6 includes the high-resolution spectra of the C-H stretching frequencies at each of the fundamental wavelengths. Considering the 532-nm data for the moment, the C-H stretching region can be modeled as a sum of seven Lorentzian bands with 21 parameters being required, i.e. relative shift, band width and height for seven bands. Of these, the band maxima of 3 transitions are well known and are used here to fix the absolute positions of all remaining transitions. Additionally, the widths were found to be similar for all the transitions concerned and thus the widths were set to a constant value; reducing the

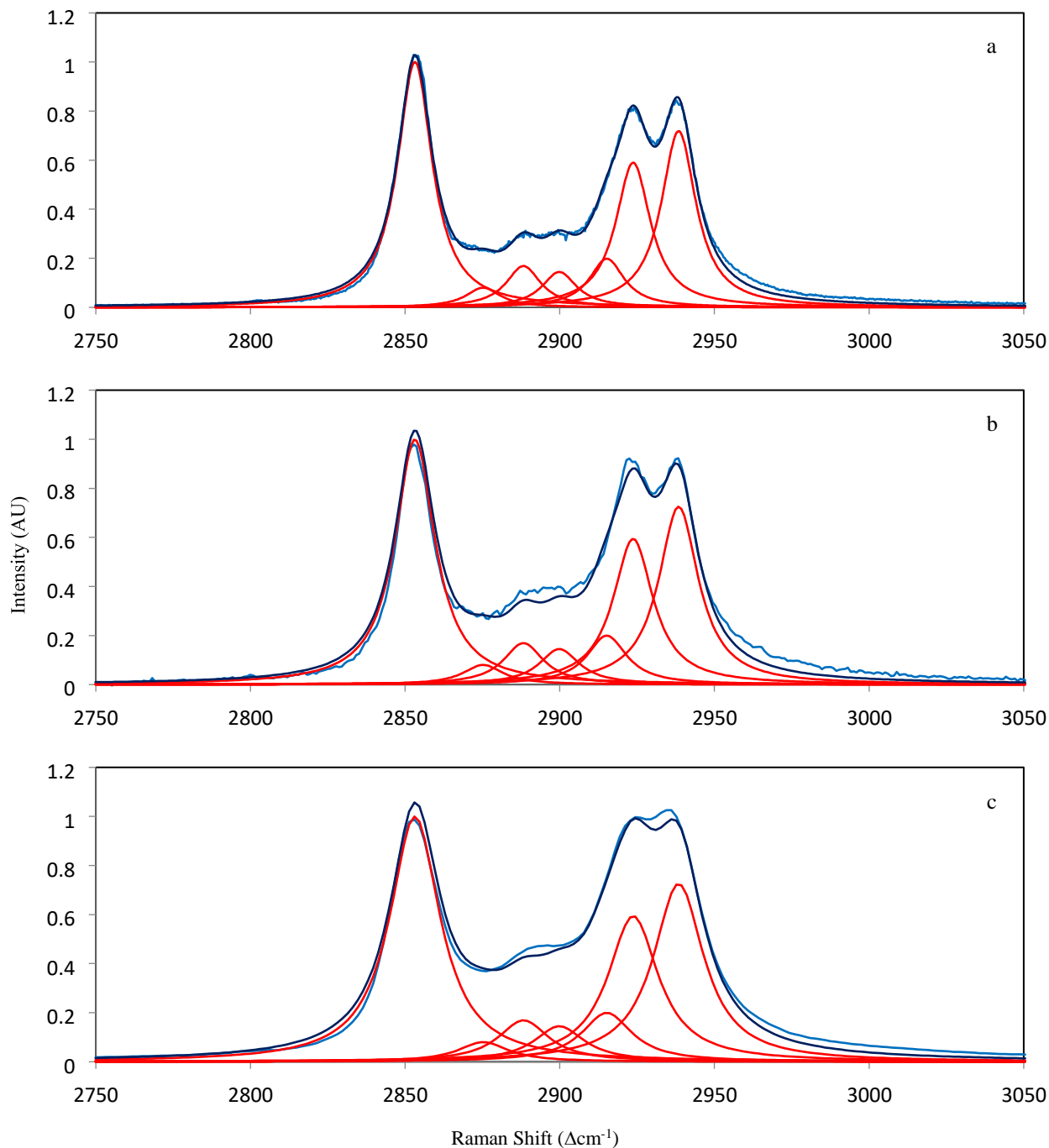


Figure 6. Raman spectra of cyclohexane collected with (a) 532 nm, (b) 266 nm, and (c) 213 nm excitation. Simulated spectra (black) were fitted to the measured spectra (blue) based on a series of Lorentzian distributions (red). Please see text for details.

number of parameters to 12. The seven individual Lorentzian contributions are included in the figure as is the sum of these contributions. The agreement between the simulated and observed data is quite good. The parameters used to achieve this fit are collected in Table 2.

Table 2. Raman shifts (Δcm^{-1}), relative intensities, and full-width-half-maximums (FWHM) of each vibrational mode corresponding to the fit performed using 532-nm excitation.

i	ν_i (cm^{-1})	Intensity (rel)	FWHM (cm^{-1})
1	2938	0.719	13.65
2	2924	0.590	13.65
3	2915	0.198	13.65
4	2900	0.144	13.65
5	2888	0.169	13.65
6	2857	0.080	13.65
7	2853	1.00	13.65

The middle spectrum shown in Figure 6 is the observed Raman spectrum of cyclohexane observed using 266-nm excitation. The similarities between this spectrum and that obtained using 532-nm excitation are clear. The 266-nm spectrum was again fit to a series of seven Lorentzian bands including the following constraints. In this case, the absolute shift positions were fixed to those obtained using 532-nm excitation, and the band heights were calculated using the standard ν_0^4 frequency dependence according to the shifts and heights obtained in the 532-nm spectrum using equation 1. The band width used were again similar for all transition observed but were slightly larger due to the changes in spectrograph dispersion at the two wavelengths regions. Thus, the band width was the only adjustable parameter and its increase was due to the decreased resolution when monitoring in the UV spectral range. The individual Lorentzian contributions, as well as the sum to these contributions, are again included in Figure 4. The fit is remarkably good as expected if resonance enhancements are not present.

The lower spectrum in Figure 6 was recorded using 213-nm excitation. The C-H stretching region is again similar to those shown in the upper and middle spectra. The spectrum can be simulated using the seven Lorentzian bands, keeping the absolute positions constant while fixing the bands heights assuming the standard ν_0^4 frequency dependence and allowing only the width to vary as above in the case of 266-nm excitation. The individual contributions of the seven Lorentzian bands, along with their sum, are also included in the figure. The Raman active C-H stretches for cyclohexane are either a_{1g} or e_g symmetry such that resonance contributions into these bands would necessarily be distributed differently into these bands. Instead, the fit is remarkably precise. For this spectrum to be reproduced using the parameter set obtained from the 532-nm spectrum, where resonance enhancement does not occur, is strong evidence that resonance enhancement does to contribute to the 213-nm spectrum either. We conclude that resonance enhancement is not occurring in the 213-nm spectrum.

CONCLUSION

A new optical arrangement for measuring UV-Raman spectra of liquid or solid samples was described. From the prospective of analytical detection and the possibility of calibrating UV Raman spectrographic system for accurate measurement of spectra, including both frequency and relative cross-sections, cyclohexane is a likely candidate for use as a secondary standard. It appeared that the anticipated enhancements due to resonance effects are not present in this sample. Evaluation of additional possible secondary standards is needed, particularly in the frequency ranges that are not covered by cyclohexane normal modes. Further investigations into the benefits of the specific configuration described here using additional solid analytes and substrates, stand-off detection and different wavelengths for excitation and are currently underway.

ACKNOWLEDGEMENTS

The authors wish to acknowledge support of this work through a UMBC/ARL CRADA under ARL ECBC JSW 1410C for work completed at UMBC. L.S. is grateful for support obtained through the National Science Foundation Research Experience for Undergraduates (NSF REU) Award No. CHE-1460653.

REFERENCES

- 1) Kullander, F.; Landström, L.; Lundén, H.; Wästerby, P. Experimental Examination of Ultraviolet Raman Cross Section of Chemical Warfare Agent Simulants. *Proc. of SPIE*. **2015**, 9455, 94550S1-9.
- 2) Kullander, F.; Landström, L.; Lundén, H.; Mohammed, S.; Olofsson, G.; Wästerby, P. Measurements of Raman Scattering in the Middle Ultraviolet Band from Persistent Chemical Warfare Agents. *Proc. of SPIE*. **2014**, 9073, 90730C1-11.
- 3) Svanqvist, M.; Nordberg, M.; Östmark, H. Single-Shot Stand-Off Detection of Explosives Precursors Using UV Coded Aperture Raman Spectroscopy. *Proc. of SPIE*. **2015**, 9455, 94550Q1-7.
- 4) Bykov, S. V.; Mao, M.; Gares, K.L.; Asher, S.A. Compact Solid –State 213 nm Laser Enables Standoff Deep Ultraviolet Raman Spectrometer: Measurements of Nitrate Photochemistry. *Appl. Spectrosc.* **2015**, 69, 895-901.
- 5) Lamsal, N.; Sharma, S. K.; Acosta, T. E.; Angel, S.M. Ultraviolet Stand-off Raman Measurements Using a Gated Spatial Heterodyne Raman Spectrometer. *Appl. Spectrosc.* **2016**, 70, 666-675.
- 6) Kim, H.; Kosuda, K. M.; Van Duyne, R.P.; Stair, P. C. Resonance Raman and Surface – and Tip – Enhanced Raman Spectroscopy Methods to Study Solid Catalysts and Heterogeneous Catalytic Reactions. *Chem. Soc. Rev.* **2010**, 39, 4820-4844.
- 7) Kelley, A.M. Resonance Raman and Resonance Hyper-Raman Intensities: Structure and Dynamics of Molecular Excited States in Solution. *J. Phys. Chem. A*. **2008**, 112, 11975-11991.
- 8) Asher, S.A. UV Resonance Raman Spectroscopy for Analytical, Physical, and Biophysical Chemistry. *Anal. Chem.* **1993**, 65, 59-66.
- 9) Myers, A.B.; Mathies, R.A. Resonance Raman Intensities: A Probe of Excited-State Structure and Dynamics. In *Biological Applications of Raman Spectroscopy*; Spiro, T. G., Ed.; John Wiley and Sons Inc.: Canada, 1987; Vol. 2, pp. 1-58.
- 10) McCreery, R. L. Photometric Standards for Raman Spectroscopy. In *The Handbook of Vibrational Spectroscopy*; Chalmers, J. M.; Griffiths, P. R., Eds.; John Wiley & Sons Ltd, United Kingdom, 2002; Vol. 1, pp. 320-332.
- 11) Tsubomura, H.; Mulliken, R. S. Molecular Complexes and their Spectra. XII. Ultraviolet Absorption Spectra Caused by the Interaction of Oxygen with Organic Molecules. *J. Amer. Chem. Soc.* **1960**, 82, 5966-5974.
- 12) Stenberg, V. I.; Olson, R. D.; Wang, C. T.; Kulevsky, N. The Role of Charge-Transfer Complexes in the Photooxidation of Ethers with Oxygen. *J. Org. Chem.* **1967**, 32, 3227-3229.
- 13) Waterland, M. R.; Meyers Kelley, A. Far-Ultraviolet Resonance Raman Spectroscopy of Nitrate ion in Solution. *J. Chem. Phys.* **2000**, 113, 6760-6773.
- 14) Trulson, M.O.; Mathies, R.A. Raman Cross Section Measurements in the Visible and Ultraviolet Using an Integrating Cavity: Application to Benzene, Cyclohexane, and Cacodylate. *J. Chem. Phys.* 1985, 82, 2068-2074.
- 15) Li, B.; Myers, A. B. Absolute Raman Cross Sections for Cyclohexane, Acetonitrile, and Water in the FarUltraviolet Region. *J. Phys. Chem.* **1990**, 94, 4051-4054.